

Nano-Ni addition to MgB₂: effects on the superconducting properties

O. F. de Lima · K. B. Vieira · E. Moschim ·
V. P. S. Awana · H. Kishan

Received: 13 October 2009 / Accepted: 4 March 2010 / Published online: 18 March 2010
© Springer Science+Business Media, LLC 2010

Abstract Samples of MgB₂ pure phase, with Ni nanoparticles addition, were prepared using a solid diffusion reaction method. Clearly, the Ni nanoparticles act as effective pinning centers and enhance the critical current density values, especially for a sample with 0.5%Ni. A negligible amount of Ni diffuses inside the MgB₂ grains, thus having a small effect on the transition temperature, which remains around 37.5 K.

Introduction

Since the discovery of superconductivity in MgB₂ [1], several studies have explored possible ways to improve its properties, like the critical current density (J_c), in small samples as well as long wires [2–4]. The relatively small anisotropy of the superconducting properties [5, 6] and the simple preparation of good samples [2] provided strong motivations towards MgB₂ applications. However, it was quickly established that effective pinning centers had to be added into the material microstructure [7], in order to halt the intense dissipation produced by flux movements.

The MgB₂ coherence length $\xi_0 = 5$ nm (at $T = 0$ K) [2, 6] allows the use of most commercially available

nanoparticles as pinning centers, since they can fit effectively in a vortex core diameter of size 2ξ , where [8] $\xi = \xi_0(1 - T/T_c)^{-1/2}$. In fact, several studies have been published [9–16] showing favorable effects of nanoparticles additions to the MgB₂ compound. The best results reported so far are due to SiC nanoparticles addition, which can improve substantially the $J_c(H)$ performance associated with an increase of the irreversibility field (H_{irr}) [9–11].

In this paper we analyze the pinning of vortex lines and the effects on J_c , in MgB₂ samples that contain small amounts of Ni nanoparticles (nano-Ni), with sizes in the range of 5–20 nm including a thin NiO layer that ranges from 0.5 to 1.5 nm in thickness [17]. In this case, besides the fact of particle sizes matching vortex cores, we also expect a stronger interaction due to magnetic pinning [13, 16].

Samples preparation and characterization

Initially, the pure MgB₂ compound was prepared from a stoichiometric mixture of Mg and B powders that were pressed and reacted in a furnace for 5 h at 800 °C, under argon atmosphere. This cycle was repeated two more times, after grinding and milling the reacted material. Next, five samples were prepared by milling and mixing the reacted material with a nano-Ni powder, using mass fractions of 0.5%, 1%, 2%, 3%, and 5%. Finally, each MgB₂ + $x\%$ Ni sample was pressed and sintered into the shape of a small bar, in a furnace at 800 °C, for 5 h, under argon atmosphere.

X-Ray Diffraction (XRD) analysis was done in all samples, using CuK α radiation. The diffractograms shown in Fig. 1 attest the good quality of all samples, with practically all peaks belonging to the pure MgB₂ phase (0%Ni). A few small impurity peaks were indexed to MgO ($2\theta =$

O. F. de Lima (✉)
Instituto de Física Gleb Wataghin, Unicamp, Campinas, SP
13083-970, Brazil
e-mail: delima@ifi.unicamp.br

K. B. Vieira · E. Moschim
Faculdade de Engenharia Elétrica e Computação, Unicamp,
Campinas, SP 13083-970, Brazil

V. P. S. Awana · H. Kishan
National Physical Laboratory, Dr. K. S. Krishnan Marg, New
Delhi 110012, India

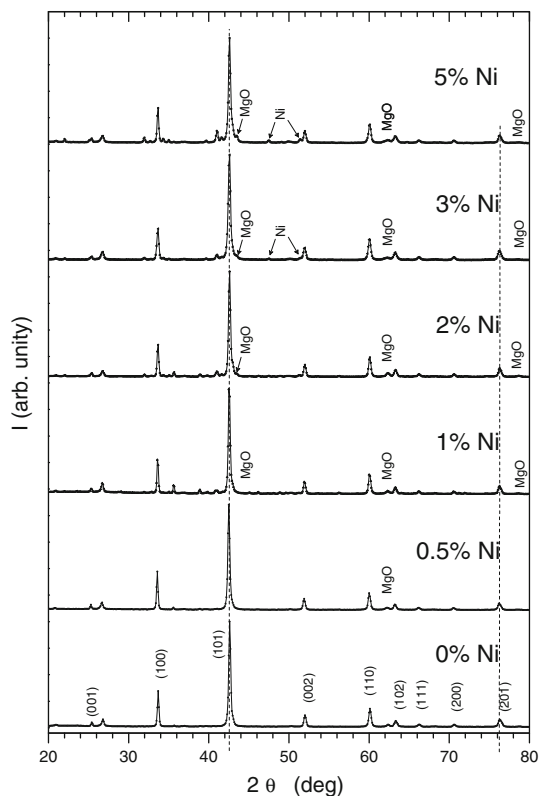


Fig. 1 X-ray diffraction patterns measured at $T = 300$ K. A few small impurity peaks were indexed to MgO ($2\theta = 43.5^\circ$, 62.4° , and 78.7°) and Ni ($2\theta = 44.4^\circ$ and 51.7°). The two vertical dashed lines indicate undetectable changes in the MgB₂ lattice parameters, due to nano-Ni addition

43.5° , 62.4° , and 78.7°), to Ni ($2\theta = 44.4^\circ$ and 51.7°) and some unknown peaks appear at $2\theta = 26.7^\circ$, 32.0° and 41.0° . We were not able to find any compound involving any combination of the candidate elements Ni, Mg, B, and O that could match the unknown peaks. Our search was performed using the Metals Database CRYSTMET (Version 4.3.0), from Toth Information Systems, Inc. The very small peaks indexed to pure Ni are clearly seen only for the samples with $x \geq 3\%$ Ni. This could be explained by the fact that most of the nano-Ni powder is delivered in an amorphous state [17], and the reaction and sintering annealings were done at the temperature of 800°C , much less than the nano-Ni melting point ($T_m = 1455^\circ\text{C}$) [17].

Energy dispersive scanning electron microscopy (ED-SEM) was employed to observe the grains morphology in the fractured surface of the samples, as shown in Fig. 2, for sample MgB₂ + 5%Ni. The matrix is porous and the grain linear size (d) is typically around $5\ \mu\text{m}$ for all samples. A similar porous structure was reported recently [18] for in situ processed MgB₂, reacted at 800°C . This was attributed to a possible Kirkendall mechanism (difference in the diffusivity between Mg and B), combined with possible capillary movement of melted magnesium [18].

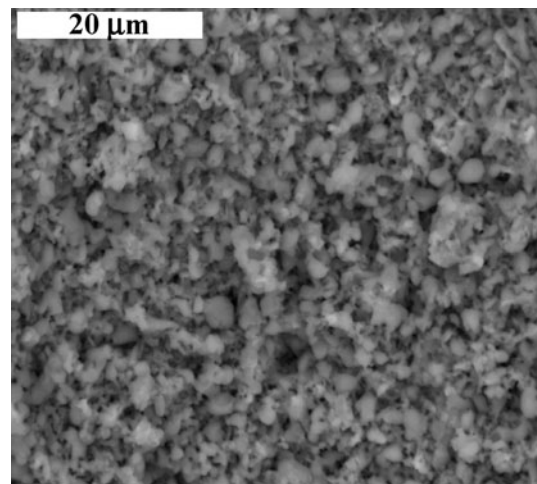


Fig. 2 ED-SEM photograph from a fractured surface of sample MgB₂ + 5%Ni

In this study, we are especially motivated to explore the effect on pinning strength, due to the nano-Ni addition, at high fields and at temperatures closer to T_c . A good parameter to evaluate quantitatively this effect is the critical current density (J_c) calculated through Bean's Critical State Model [19]:

$$J_c(H) = \frac{30 * |\Delta M|}{d} \quad (1)$$

where $|\Delta M|$ is the width of the magnetization hysteresis loop, and d is an average of the linear size of sample grains. Although Eq. 1 is derived for an infinite cylinder of diameter d , it also produces useful estimates of J_c for granular samples. In this work, we have used $d = 5\ \mu\text{m}$ and $|\Delta M|$ values extracted directly from the $M(H)$ curves.

Results and discussion

Figure 3a reveals narrow magnetic transitions between the normal and superconducting states, around $T_c = 37.5$ K, for all MgB₂ + $x\%$ Ni samples. The pure MgB₂ sample presented the highest $T_c = 38$ K, which is close to the value of 39 K expected for a pure phase [1]. In Fig. 3b one sees that T_c is weakly affected by the nano-Ni addition. The main T_c depression, reaching a maximum of about 0.9 K, happens for concentrations up to around 2%Ni. For the samples having larger Ni contents T_c oscillates around 37.1 K, with a jump to about 37.3 K for MgB₂ + 3%Ni. The error bars appearing in Fig. 3b represent the transition widths (10–90%). Our general conclusion is that only a small amount of Ni atoms actually penetrates in the MgB₂ pure grains, thus having a negligible effect on T_c .

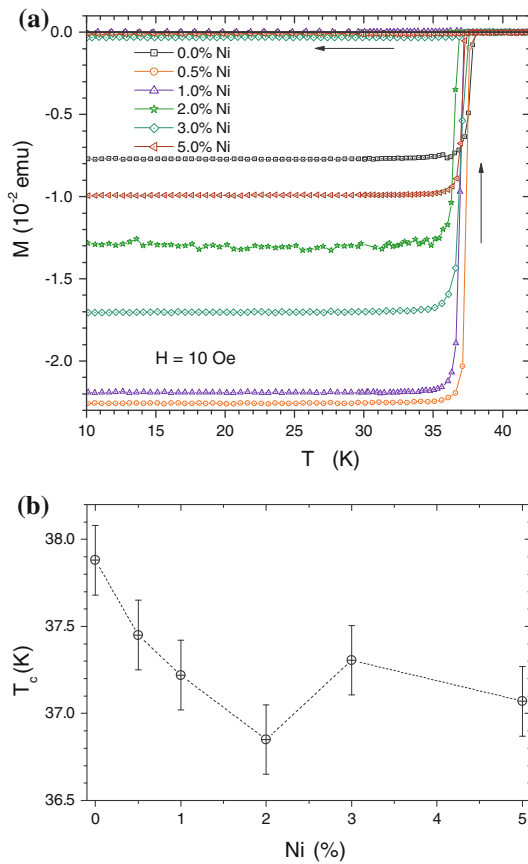


Fig. 3 **a** Magnetic moment as a function of temperature, showing sharp transitions between the normal and superconducting states around 37.5 K; **b** T_c as a function of Ni content. The error bars represent transition widths (10–90%)

We expect that almost all Ni atoms are located between MgB_2 grains, since it is known that there is only a small diffusion of Ni inside MgB_2 for $T > 980$ °C [20]. Possible second phase candidates at this high temperature region would be NiB and Mg_2Ni [21]. Therefore, in our conditions with $T = 800$ °C and small Ni contents ($x < 5\%$) we expect a very small amount of Ni dissolved in the MgB_2 matrix. Consistent with this fact all XRD peaks belonging to the MgB_2 phase fall in the same angular positions (see the vertical dashed lines in Fig. 1), independently of the Ni content, thus indicating no effect of solid solution on the MgB_2 lattice parameters. Further, none of the impurity peaks belongs to NiB or Mg_2Ni compounds.

The magnetization hysteresis loops are shown in the isothermal $M(H)$ curves of Fig. 4a, b, respectively, for $T = 5$ and 30 K. The discontinuities, or flux jumps, that occur mainly at low fields and low temperatures, are caused by thermomagnetic instabilities [7], very typical in MgB_2 . Usually these instabilities can be reduced or suppressed by strong vortex pinning, combined with the addition of large fractions of high thermal conducting

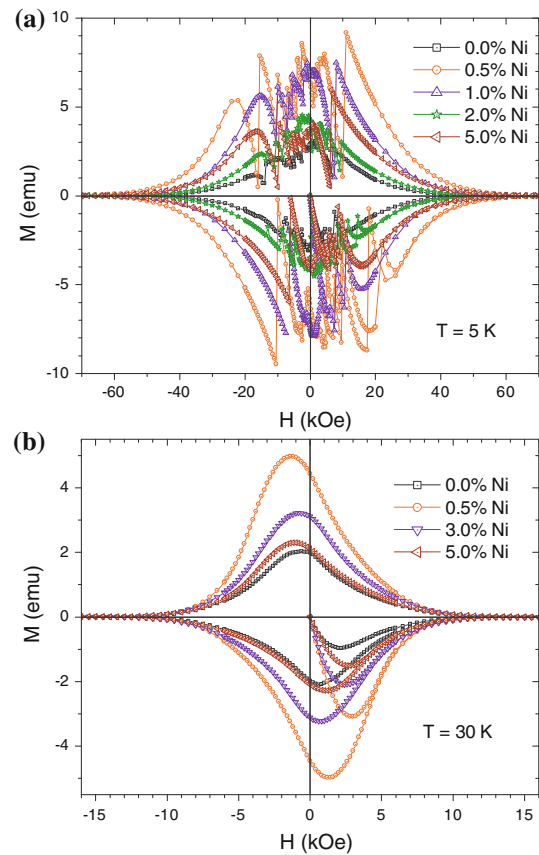


Fig. 4 Isothermal magnetization curves, measured at **a** 5 K and **b** 30 K. The discontinuities occurring at low fields for $T = 5$ K are caused by thermomagnetic instabilities

materials, like copper or silver, as typically employed in superconducting wires.

Figure 5 shows the $J_c(H)$ curves, calculated with Eq. 1, respectively for $T = 5$ and 30 K (inset). Similar curves were also obtained for $T = 10$ and 20 K, for all samples (not shown here). Figure 6 shows that as T increases the isothermal $J_c(H)$ curves becomes shifted to lower J_c values, as expected. Although Fig. 6 refers only to the sample $MgB_2 + 0.5\%Ni$, this is actually a common feature of all samples.

Clearly, the nano-Ni addition to MgB_2 enhances the $J_c(H)$ performance, with the best results occurring for the sample with 0.5%Ni. This concentration possibly represents the best compromise between a favorable magnetic pinning of vortices and an unfavorable depression of T_c . Both factors are known to influence the pinning force [22], which is directly related to J_c . Relatively high J_c values were observed for sample $MgB_2 + 0.5\%Ni$; one example is $J_c = 1.3 \times 10^6$ A/cm² at $T = 5$ K and $H = 20$ kOe. We found also that the performance of sample $MgB_2 + 3\%Ni$ was slightly better than the 0.5%Ni sample, as seen in the inset of Fig. 5 especially for $H > 5$ kOe. This is an

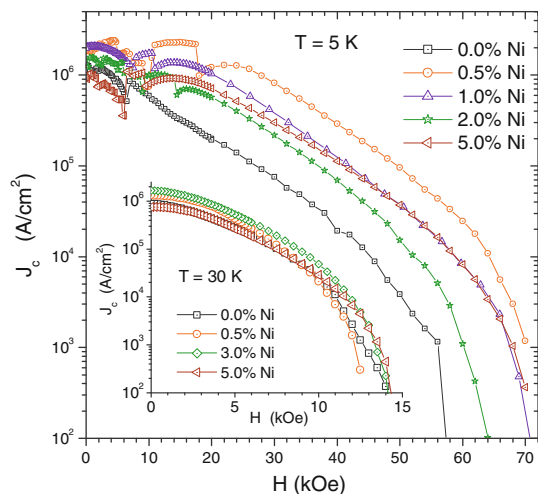


Fig. 5 Critical current density as a function of applied field, calculated with Bean's model, for $T = 5$ and 30 K (inset)

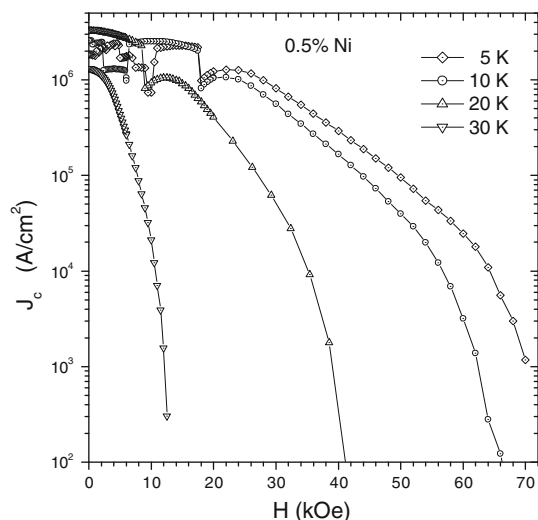


Fig. 6 Critical current density as a function of applied field, for sample $\text{MgB}_2 + 0.5\% \text{Ni}$, calculated at several temperatures

unexpected behavior when comparing with all the other samples. Searching for a possible cause, we found that the 3%Ni sample has a specific mass of 1.27 g/cm^3 , about 11% higher than the observed for the other samples (1.14 g/cm^3), possibly due to some adverse processing parameter. Therefore, sample $\text{MgB}_2 + 3\% \text{Ni}$ possibly has a better connectivity between its grains, favoring higher induced J_c values.

Comparing our results for the sample $\text{MgB}_2 + 0.5\% \text{Ni}$ with the literature, at $T = 5 \text{ K}$ and $H = 60 \text{ kOe}$ we have $J_c = 2.6 \times 10^4 \text{ A/cm}^2$, while for the best sample with nano- TiO_2 addition [15] it was found $4 \times 10^3 \text{ A/cm}^2$, and for the best sample with nano- SiC addition [9, 11] it was found $\sim 10^5 \text{ A/cm}^2$. Extending the comparisons to other T and H values we conclude that our best results for J_c are

roughly four times below the best results in the literature for nano- SiC addition, and at least six times above the best results for nano- TiO_2 addition.

Conclusions

Pure phase MgB_2 was prepared using a solid diffusion reaction method, starting from a mixture of Mg and B powders. Several samples were obtained by milling, mixing, and sintering the reacted MgB_2 with different contents of nano-Ni powder. Sharp transitions to the superconducting state were observed with relatively high critical temperatures (T_c) near 37.5 K. The nano-Ni addition had a limited effect on T_c , producing a maximum depression of about 0.9 K for concentrations around 2%Ni. On the other hand, the nano-Ni addition to MgB_2 clearly enhanced the critical current density (J_c), with the best results occurring for the sample with 0.5%Ni. Our best values for J_c (e.g., $2.6 \times 10^4 \text{ A/cm}^2$ at $T = 5 \text{ K}$ and $H = 60 \text{ kOe}$) are roughly four times below the best results found in the literature for nano- SiC addition [9, 11], and more than six times above the best results for nano- TiO_2 addition [15].

Acknowledgements The authors would like to thank the technical staff from the Geosciences Institute of Unicamp for the SEM work, and the technical staff from the LIEC/UNESP/Araraquara for the AFM and MFM images. O. F. de Lima, K. B. Vieira and E. Moschim acknowledge the financial support from Brazilian Science Agencies Fundação de Amparo à Pesquisa do Estado de São Paulo (FAPESP), Conselho Nacional de Desenvolvimento Científico e Tecnológico (CNPq) and Coordenação de Aperfeiçoamento de Pessoal de Nível Superior (CAPES). V. P. S. Awana and H. Kishan acknowledge the interest and advice given by Prof. Vikram Kumar from National Physical Laboratory, N. Delhi.

References

1. Nagamatsu J, Nakagawa N, Muranaka T, Zenitani Y, Akimitsu J (2001) Nature 410:63
2. Canfield PC, Bud'ko SL, Finnemore DK (2003) Physica C 385:1
3. Collings EW, Sumption MD, Bhatia M, Susner MA, Bohnenstiehl SD (2008) Supercond Sci Technol 21:103001
4. Nakane T, Takahashi K, Kitaguchi H, Kumakura H (2009) Physica C 469:1531
5. de Lima OF, Ribeiro RA, Avila MA, Cardoso CA, Coelho AA (2001) Phys Rev Lett 86:5974
6. de Lima OF, Cardoso CA, Ribeiro RA, Avila MA, Coelho AA (2001) Phys Rev B 64:144517
7. Bugoslavsky Y, Cohen LF, Perkins GK, Polichetti M, Tate TJ, Gwilliam R, Caplin AD (2001) Nature 411:561
8. Tinkham M (1996) Introduction to superconductivity. McGraw-Hill, New York
9. Dou SX, Soltanian S, Horvat J, Wang XL, Munroe P, Zhou SH, Ionescu M, Liu HK, Tomsic M (2002) Appl Phys Lett 81:3419
10. Yeoh WK, Dou SX (2007) Physica C 456:170
11. Dou SX, Shcherbakova O, Yeoh WK, Kim JH, Soltanian S, Wang XL, Senatore C, Flukiger R, Dhalle M, Husnjak O, Babic E (2007) Phys Rev Lett 98:097002

12. Cheng CH, Zhang H, Zhao Y, Feng Y, Rui XF, Munroe P, Zeng HM, Koshizuka N, Murakami M (2003) *Supercond Sci Technol* 16:1182
13. Snezhko A, Prozorov T, Prozorov R (2005) *Phys Rev B* 71:024527
14. Awana VPS, Isobe M, Singh KP, Takayama-Muromachi E, Kishan H (2006) *Supercond Sci Technol* 19:551
15. Kishan H, Awana VPS, de Oliveira TM, Alam S, Saito M, de Lima OF (2007) *Physica C* 458:1
16. Qu B, Sun XD J-G, Li J-G, Xiu ZM, Liu SH, Xue CP (2009) *Supercond Sci Technol* 22:015027
17. Quantum Sphere (2007) Specifications sheet for QSI-nano nickel. USA
18. Yi JH, Kim KT, Jun B-H, Sohn JM, Kim BG, Joo J, Kim C-J (2009) *Physica C* 469:1192
19. Bean CP (1964) *Rev Mod Phys* 36:31
20. Suo HL, Beneduce C, Dhallé M, Musolino N, Genoud J-Y, Flükiger R (2001) *Appl Phys Lett* 79:3116
21. Elliott RP (1965) *Constitution of binary alloys*, first supplement. McGraw-Hill, Inc, New York
22. Blatter G, Feigel'man MV, Geshkenbein VB, Larkin AI, Vinokur VM (1994) *Rev Mod Phys* 66:1125